ELSEVIER

Thermochimica Acta 308 (1998) 77–83

thermochimica acta

Calorimetric investigation of the behavior of interlamellar water in phospholipid–water systems[1]

Hiroyuki Aoki, Michiko Kodama*

Department of Biochemistry, Faculty of Science, Okayama University of Science, 1-1 Ridai-cho, Okayama 700, Japan

Received 15 October 1996; received in revised form 7 February 1997; accepted 13 February 1997

Abstract

The interaction of water and three phospholipids with different polar-head groups, phosphatidylethanolamine (PE), phosphatidylcholine (PC) and phosphatidylgylcerol (PG) were investigated by differential scanning calorimetry (DSC). Ice-melting DSC curves showed that two types of water molecules, nonfreezable and freezable, interacting with lipid-head groups in intra-, and inter-bilayers are present in the gel phase of three lipid–water systems of varying water content up to 40 g%. The ice-melting curves were deconvoluted according to a computer program and the number of bulk water molecules and subsequently the number of nonfreezable and freezable interlamellar water molecules was estimated from enthalpy changes of deconvoluted components. The number of nonfreezable interlamellar water molecules increased in the order of PE (2.3 H_2O/lipid, PG (4.0 H_2O/lipid) and PC (5.5 H_2O/lipid), that is, in the order of an increase in the effective area occupied by the three-head groups. However, a distinct difference was observed for the freezable interlamellar water: the number of this water molecules of PG system continuously increases up to 40 g%, in contrast with their limiting number of 3.7 and 4.5 H_2O/lipid for PE and PC systems, respectively. This difference accounted well for a difference in the multiplicity of bilayer lamellar, that is, a single lamellar for PG system and a multilamellar for PE and PC systems shown by electron microscopy. © 1998 Published by Elsevier Science B.V.

Keywords: Differential scanning calorimetry; Electron microscopy; Interlamellar water molecules; Phospholipid–water systems

1. Introduction

Phospholipids, main components of biomembranes, constitute their fundamental bilayer structure. There are a great variety of phospholipids in biomembranes but a specific composition of these lipids is observed in different types of membranes. From this viewpoint, attention of many investigators has been paid to the specificity of bilayer structure in lipids of different polar-head groups. In this connection, our previous papers [1] have revealed a distinct structural difference among three homologous dimyristoyl (DM) lipids of different head groups, phosphatidylethanolamine (PE), phosphatidylcholine (PC) and phosphatidylgylcerol (PG). Thus, as shown by electron micrographs in Fig. 1, the PE and PC, neutral lipids, constitute multilamellar assemblies consisting of the

*Corresponding author. Tel.: 0081 86 252 3161; fax: 0081 86 255 7700.

[1]Presented at the 14th IUPAC Conference on Chemical Thermodynamics, held in Osaka, Japan, 15–30 August, 1996.

PII S0040-6031(97)00334-1

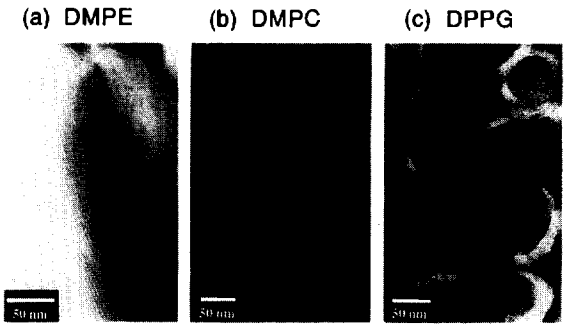

Fig. 1. Negative stain-electron micrographs of (a) DMPE-, (b) DMPC- and (c) DPPG–water systems.

lipid bilayers and interlamellar water layers, although there is a difference in the surface curvature of both bilayers, planar and spherical. In this contrast, a single lamellar assembly of highly curved surface is observed for the negatively charged PG [2]. These structural differences are related to a difference in the interactions not only of lipid–lipid but also of lipid–water among three lipids. These interactions are intimately correlated to each other. For example, in a case of PE which is a typical hydrogen-bonding lipid, the intermolecular hydrogen-bonding formed between amino and phosphate groups of adjacent lipids induces a less hydration of their head groups [3,4]. On the other hand, for PG, a continuous incorporation of water molecules between the negatively charged bilayers could be predicted [5].

From this viewpoint, in the present study, the difference in the interaction of three lipids of PE, PC and PG with water molecules in the gel phase was investigated by differential scanning calorimetry (DSC). Based upon deconvolution analyses of the ice-melting DSC curves, the number of water molecules interacting with these lipids was estimated. Structural information of lipid self-assemblies was obtained by negative-stain electron microscopy.

2. Materials and methods

1,2-dimyristoyl-3-*sn*-phosphatidylethanolamine (DMPE), 1,2-dimyristoyl-3-*sn*-phosphatidylcholine (DMPC) and 1,2-palmitoyl-*sn*-glycero-3-[phospho-*rac*-(1-glycerol)](DPPG, sodium salt) were purchased from Sigma and used without further purification, as thin-layer chromatography of each lipid showed a single spot. Each lipid, which was transferred to the high-pressure crucible cell of a Mettler differential scanning calorimeter (TA-4000), was dehydrated under high vacuum (10^{-4} Pa) at room temperature for at least 3 days until weight loss was not detected by a Chan electrobalance. The crucible cell containing the dehydrated lipid was sealed off in a dry box filled with dry N_2 gas and then weighed by a microbalance (Mettler M3). Samples of the DMPE-, DMPC- and DPPG–water mixtures ranging, in water content, from 0 to about 40 g% were prepared by successive additions of desired amounts of water to each dehydrated lipid (ca. 50 mg) by using a microsyringe. Thus, for a series of samples of different water contents, the weight of lipid is always the same and only the weight of water is different. The water contents were ascertained by weighing the sample and the cell. All the samples were annealed by repeating thermal cycling at temperatures above and below the transition to the liquid-crystal phase to ensure homogeneous mixing, until the same transition peak was attained. After that, the samples were cooled to −80°C for the DSC.

DSC measurements were carried out with a Mettler TA-4000 apparatus by placing the sample in a high-pressure crucible (pressure resistant to 100 kP/cm^2) and heating it from −80°C to temperatures of the liquid-crystal phase at a heating rate of 1.0°C/min.

Ice-melting DSC curves were analyzed by a deconvolution method according to a computer program ORIGIN (Microcal Software) for Gaussian curve analysis. In the deconvolution analyses, both the half-height width and the midpoint temperature of each of deconvoluted curves for the same sample were nearly fixed throughout all the deconvolutions. A sum of deconvoluted curves, i.e., a theoretical curve was well fitted to experimental DSC curve up to 40 g% water content investigated with standard deviations of 0.4–1.2 kJ K^{-1} mol^{-1}. However, above this water content, the standard deviation becomes larger with an increase in water content because large amount of water, very likely existing in bulk water, causes the DSC curve to stretch its foot to a high-temperature side.

Negative-stain electron microscopic experiments with sodium phosphotungstate (pH≈7) were performed with a JEOL JEM-2000EX electron microscopy operated at 200 kV at around 20°C.

3. Results and discussion

PG of a dimyristoyl-chain, DMPG, shows a faint peak due to a transition of crystalline-to-gel phases, the temperature of which is decreased to a ice-melting temperature region with increasing water content (data not shown). Therefore, in the present study, DPPG was used in place of DMPG, based upon the information that the chain-length effect on the interaction between lipid-head groups and water molecules is little [6]. Fig. 2 shows a series of ice-melting DSC curves for the gel phase of DMPE (A)-, DMPC (B)- and DPPG (C)–water systems of varying water content up to ca. 35 g%. All the samples were heated immediately after they were cooled from temperatures of the liquid-crystal phase to −80°C. In Fig. 2, a similar water-content dependence of ice-melting behavior is observed for the three systems. Thus, no ice-melting peak is observed at a low-water content. However, above boundary water contents of 8, 14 and 12 g% for DMPE, DMPC and DPPG systems, respectively, a broad ice-melting peak begins to grow over a wide temperature range below 0°C. With a further increase in water content, the broad ice-melting peak is followed by a sharp one at around 0°C. Such common ice-melting behavior suggests that in the gel phase of lipid–water systems, there are, on the whole, three types of water molecules, that is, nonfreezable and freezable water molecules bound to lipid-head groups and bulk water molecule. The nonfreezable water molecule, that is, tightly-bound water molecule is considered to exist in a bilayer and/or at the bilayer surface and interact directly with the head groups. In this comparison, the freezable water molecule characterized by the broad ice-melting peak is suggested to be loosely bound to the head groups, although the water molecule exists between lamellae. The bulk water molecule exists outside lamellae. When the broad ice-melting peaks shown in Fig. 2 are compared among the three systems of nearly the same water content, the shape and starting temperature of these peaks are different, indicating different bonding modes of the freezable interlamellar water molecule in these systems.

In order to estimate the enthalpy change due to a melting of each of frozen interlamellar water and frozen bulk water, the ice-melting DSC curves shown in Fig. 2 were deconvoluted according to a computer

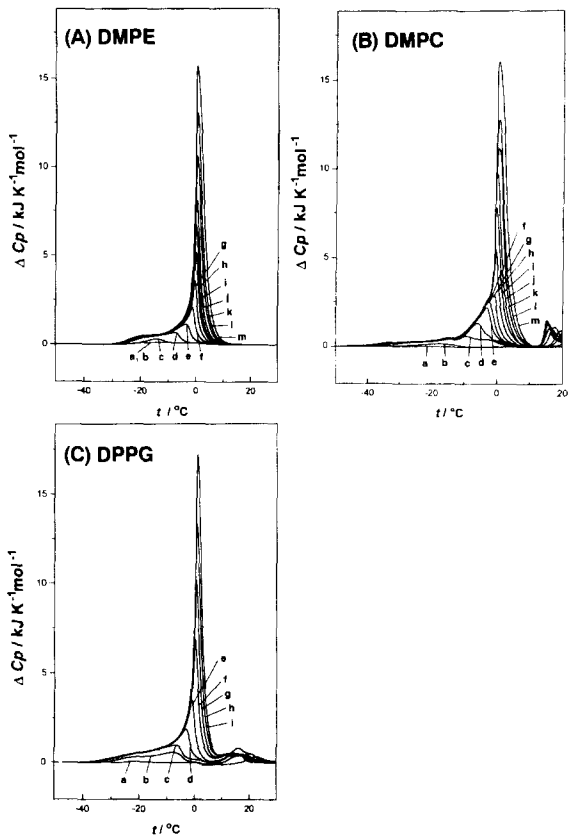

Fig. 2. Comparison of a series of ice-melting curves in gel phases of (A) DMPE-, (B) DMPC- and (C) DPPG–water systems of varying water content. Apparent, excess heat capacity (ΔC_p) per 1 mol of each lipid is plotted against temperature (t). Water contents (g%) of DMPE(A)-, DMPC(B)- and DPPG(C)–water systems: (A) (a) 2.25, (b) 6.0, (c) 8.0, (d) 10.2, (e) 12.2, (f) 14.1, (g) 16.1, (h) 18.1, (i) 20.0, (j) 22.0, (k) 25.0, (l) 28.0, (m) 32.0; (B) (a) 12.3, (b) 14.2, (c) 16.2, (d) 17.8, (e) 19.1, (f) 20.1, (g) 21.2, (h) 23.1, (i) 25.1, (j) 26.9, (k) 29.0, (l) 31.1, (m) 35.1; and (C) (a) 8.1, (b) 11.9, (c) 14.1, (d) 16.0, (e) 18.0, (f) 21.1, (g) 23.9, (h) 27.0, (i) 29.9.

program ORIGIN [7,8]. Based upon resulting deconvolution data, the number of each of the nonfreezable and freezable interlamellar water molecules and bulk water molecules was estimated according to a method described below.

Fig. 3 compares results of the deconvolution analyses of the three systems at nearly the same water content, as an example. The present deconvolution analyses are based upon a way such as minimizing the total number of deconvoluted curves. In Fig. 3, the three systems likewise show a four-component decon-

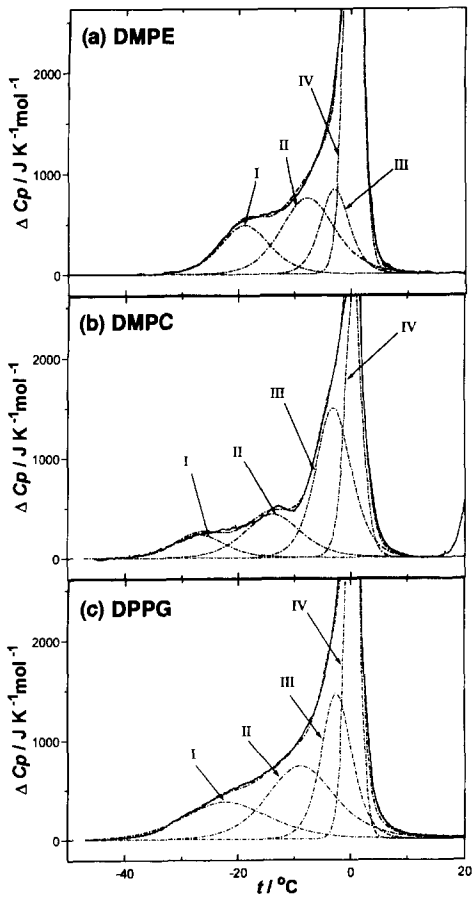

Fig. 3. Comparison of deconvolution analyses of ice-melting curves for gel phases of (a) DMPE-, (b) DMPC- and (c) DPPG–water systems. Water content (g%): (a) 22.0, (b) 21.2, (c) 21.1. The deconvolutions were performed on the basis of a computer program attached to a Microcal calorimeter [7,8]. In each figure, four deconvoluted curves I, II, III and IV as well as a theoretical curve are shown by dotted lines. The apparent, excess heat capacity (ΔC_p) per 1 mol of each lipid is plotted against temperature (t).

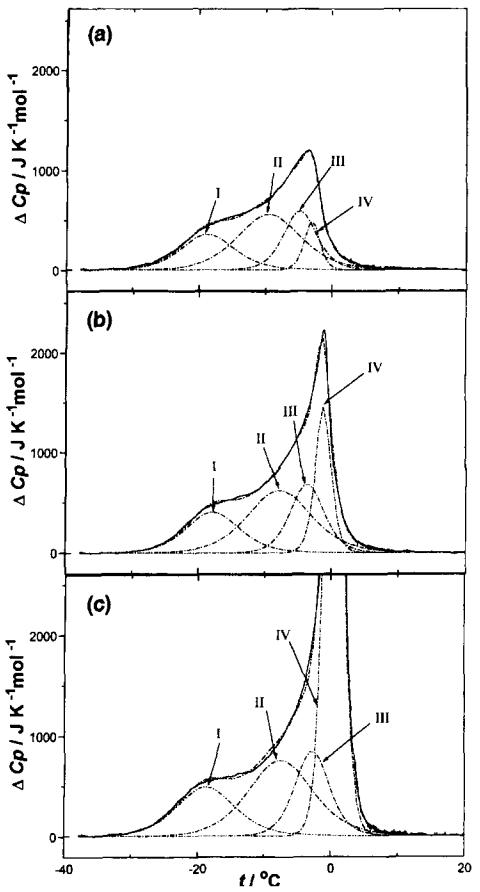

Fig. 4. Deconvolution analyses of ice-melting curves for gel phases at water contents of (a) 12.2, (b) 14.1 and (c) 22.0 g%. The deconvolutions were performed on the basis of a computer program attached to a Microcal calorimeter [7]. In each figure, four deconvoluted curves I, II, III and IV as well as a theoretical curve are shown by dotted lines. The apparent, excess heat capacity (ΔC_p) per 1 mol of DMPE is plotted as a function of temperature (t).

volution, that is, deconvoluted curves, I, II and III constituting the broad ice-melting peak, in addition to a deconvoluted curve IV comparable to the sharp ice-melting peak at 0°C. However, when these deconvoluted curves are compared among the curves of corresponding number in the three systems, the midpoint temperature as well as the half-height width differs. In this contrast, nearly the same midpoint temperature and half-height width of the corresponding curves are observed for the same lipid system of different water contents, as is evidenced by DMPE–water system in Fig. 4, as an example.

In Fig. 5, enthalpy changes ΔH_1, ΔH_2 and ΔH_3 of the deconvoluted curves I, II and III per 1 mol of lipid, together with a sum of these enthalpy changes $\Delta H_{(1+2+3)}$ are plotted against water/lipid molar ratio N_w (molar number of water molecules added to 1 mol of lipid) of a sample and are compared among the three systems (a, b and c). By extrapolating the $\Delta H_{(1+2+3)}$ versus N_w curves of these systems to a lower-water content region, the starting points of these curves are shown to be 2.3, 5.5 and 4.0 molar ratio for DMPE, DMPC and DPPG systems, respectively. Below these boundary water contents, no ice-melting

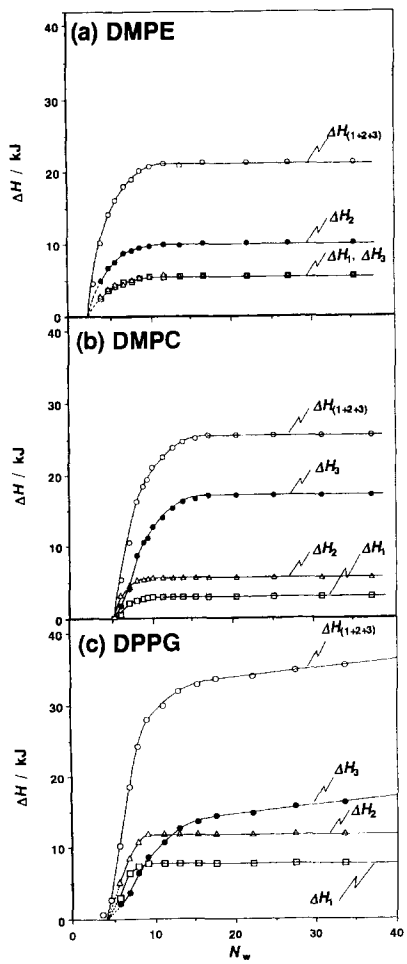

Fig. 5. Comparison of enthalpy changes ΔH_1, ΔH_2, ΔH_3 and $\Delta H_{(1+2+3)}$ of deconvoluted ice-melting curves in gel phases of (a) DMPE-, (b) DMPC- and (c) DPPG–water systems. The enthalpy changes per 1 mol of each lipid are plotted against water/lipid molar ratio (N_w). ΔH_1, ΔH_2, ΔH_3 and $\Delta H_{(1+2+3)}$ represent enthalpy changes for the deconvoluted curves I, II, III and their sum, respectively. The deconvoluted curves I, II and III were derived from freezable interlamellar water.

peak is observed for the three systems. Therefore, a maximum limiting number of nonfreezable, tightly-bound water molecules is found to be 2.3, 5.5 and 4.0 H_2O per lipid for DMPE, DMPC and DPPG systems, respectively. In a higher-water content region, the $\Delta H_{(1+2+3)}$ curves of DMPE and DMPC systems reach maxima at molar ratios of approximately 10 and 17, respectively. Thus, DMPE and DMPC systems show a limited uptake of the freezable interlamellar water, although the limiting water content is different in both systems. However, the $\Delta H_{(1+2+3)}$ curve of DPPG system continues to increase with increasing water content. This fact indicates that DPPG system incorporates the freezable water between lamellae, without limitations, up to at least 40 molar ratios investigated. When the ΔH_1, ΔH_2 and ΔH_3 curves are compared among the three systems, the difference in the $\Delta H_{(1+2+3)}$ curve is shown to arise from the ΔH_3 curve. Thus, both the ΔH_1 and ΔH_2 curves of the three systems reach maxima at nearly the same molar ratio of around 10, indicating the same water-content dependence of both curves. In this contrast, the water-content dependence of the ΔH_3 curve is different among the three systems and comparable to that of the $\Delta H_{(1+2+3)}$ curve: the ΔH_3 curves of DMPE and DMPC systems reach maxima at molar ratios of 10 and 17, respectively, and the ΔH_3 curve of DPPG system continuously increases. This result suggests a critical role of the most loosely-bound interlamellar water, which is presumed to be situated at the center of interlamellar space.

In Fig. 6, an enthalpy change ΔH_4 of the deconvoluted curve IV characterizing the bulk water is plotted against N_w of the three systems. A theoretical curve given by 6.01 N_w (6.01; molar melting enthalpy of hexagonal ice/kJ) is added in Fig. 6. The theoretical curve is based upon the assumption that all the water added to a sample is present in bulk free water. The behavior of ΔH_4 curves of the three systems is comparable to that of $\Delta H_{(1+2+3)}$ curves in Fig. 5. Thus, the ΔH_4 curves of DMPE and DMPC systems become parallel to the theoretical curve at molar ratios above 10 and 17, respectively, just corresponding to the limiting water content of the $\Delta H_{(1+2+3)}$ curve. In this contrast, the ΔH_4 curves of DPPG system shows a slope lower than that of the theoretical curve. The behavior of the ΔH_4 curve for DMPE and DMPC systems indicates that the amount of water other than the bulk water given by a difference between the theoretical and ΔH_4 curve is the same above 10 and 17 molar ratios for DMPE and DMPC systems, respectively. In the present system, the water other than the bulk water corresponds to the nonfreezable and freezable interlamellar waters, both being bound to the head groups. In order to estimate the limiting total number of these two water molecules, the straight ΔH_4 curve obtained above the limiting water content was extrapolated to a lower-water content region. The

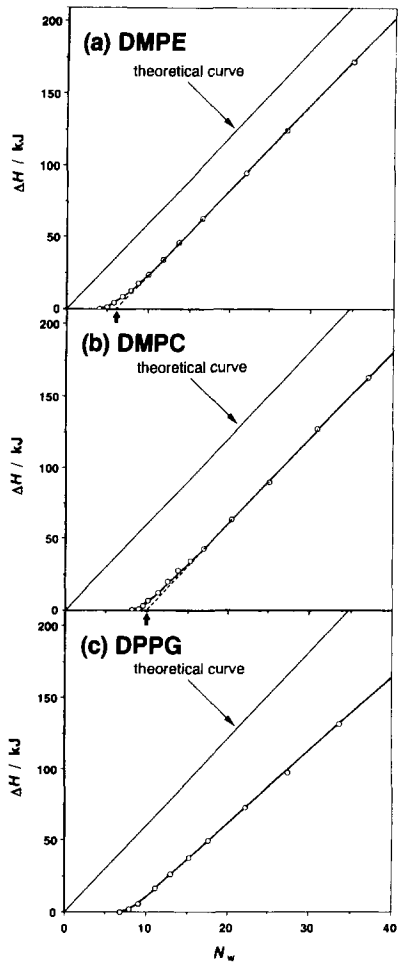

Fig. 6. Comparison of enthalpy changes ΔH_4 of deconvoluted ice-melting curve IV derived from bulk water in gel phases of (a) DMPE-, (b) DMPC- and (c) DPPG–water systems. The enthalpy change per 1 mol of each lipid is plotted against water/lipid molar ratio (N_w). In each figure, the bold line shows a theoretical curve obtained from the melting enthalpy of hexagonal ice.

extrapolated lines of DMPE and DMPC systems intersect with the abscissa at molar ratios of 6.0 and 10.0, respectively, as shown by an arrow in Fig. 6. Therefore, the limiting total number of the nonfreezable and freezable interlamellar water molecules is shown to be 6.0±0.2 and 10.0±0.2 molecules per lipid for DMPE and DMPC systems, respectively. These numbers are given with the average standard deviation of 0.2 water molecules per lipid, which was estimated from the average standard deviation of 1.2 kJ K^{-1} mol^{-1} between the theoretical and experimental curves shown in Fig. 3[7]. The limiting total numbers of 6.0±0.2 and 10.0±0.2 correspond to the maximum amount of water incorporated between the bilayers for a fully hydrated-gel phase of DMPE and DMPC systems. The limiting values of these systems fairly agree with those estimated from electron density profiles [9,10]. Based upon the limiting values, the number of the freezable interlamellar water molecules for a fully hydrated-gel phase is estimated to be 3.7±0.2 and 4.5±0.2 for DMPE and DMPC systems, respectively.

On the other hand, the difference between the theoretical and ΔH_4 curves of DPPG system becomes larger with increasing water content, indicating that the amount of the freezable interlamellar water continues to increase.

The number of each of the nonfreezable and freezable interlamellar water molecules and the bulk water molecules, $N_{n.f}$, N_f and N_b, of varying water content for the three systems was calculated according to the following equation: $N_t(=N_w)=N_{n.f}+N_f+N_b$, where N_t is the total number of water molecules added to lipid molecule. As shown in Fig. 2, the nonfreezable and freezable interlamellar waters and the bulk water appear in this order with increasing water content. Accordingly, when there is no freezable water at low-water contents, $N_{n.f}$ becomes equal to N_t. With a further increase in water content, when maximum limiting uptake of the nonfreezable water is attained, the freezable interlamellar water appears; the number of this water, N_f, is given by $N_t-(N_{n.f}+N_b)$, where $N_{n.f}$ corresponds to the limiting value (2.3, 5.5 and 4.0 for DMPE, DMPC and DPPG) estimated from Fig. 5 and N_b is obtained by dividing a value of ΔH_4 by 6.01. In Fig. 7, resulting cumulative value of $N_{n.f}$, N_f and N_b is plotted against N_w and compared among the three systems.

With reference to Fig. 7, the present results are discussed as follows:

1. The limiting number of the nonfreezable water molecules in the gel phase of the three lipid–water systems increases in the order of DMPE, DPPG, DMPC. This is concerned with a hydrogen-bond forming property of DMPE and furthermore with a smaller geometrical size of its head group, compared with other two lipids. Thus, previous X-ray crystallographic studies [11,12] have revealed that

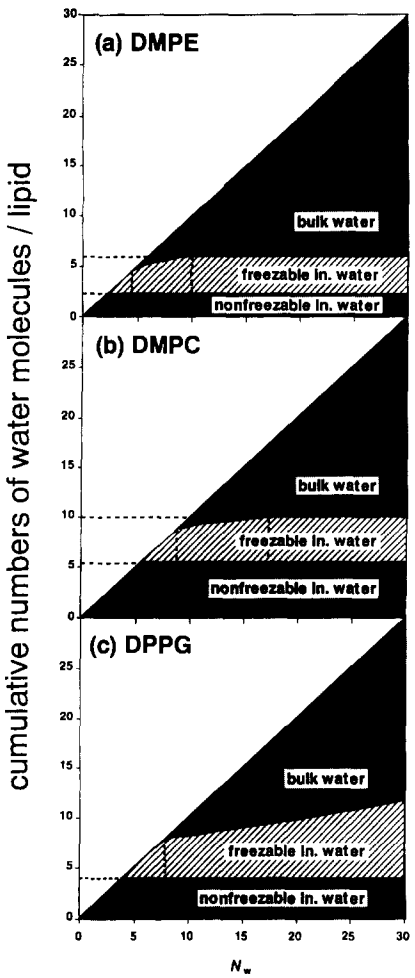

Fig. 7. Comparison of cumulative number of nonfreezable water molecules, freezable interlamellar water molecules and bulk water molecules in gel phases of (a) DMPE-, (b) DMPC- and (c) DPPG–water systems. The cumulative number is plotted against water/lipid molar ratio (N_w).

adjacent-head groups of PEs directly bind by the intermolecular hydrogen-bonding. This involves a release of water molecules from their head groups [3]. In this contrast, the PCs-head groups have been reported to be linked via a hydrogen-bond with water molecules [12]. For DPPG, its negatively-charged head groups are assumed to be linked in a way the same as that of DMPC-head groups, because a screening action of Na counter-ion (a molar ratio of $[Na^+]/[DPPG^-]=1$) on the charged-head groups is not high enough to form lipid intermolecular hydrogen-bonding [2,3]. Furthermore, considering repulsion space between adjacent DPPG-head groups, their effective size is evaluated to be larger than that predicted from their geometrical size [2]. Such a large size of both DMPC- and DPPG-head groups could provide a large space occupied by water molecules in the intrabilayer.

2. The gel phase of DPPG continuously incorporates the freezable water molecules between the bilayers, in contrast with the gel phases of the other two lipids, in which the uptake of this freezable interlamellar water is limited. This difference is concerned with electrostatic repulsion operating between negatively charged DPPG bilayer surfaces opposing each other in the interbilayer. The repulsion force depends on the distance between apposing bilayers, so that the uptake of the freezable interlamellar water continues with a direction to minimizing its force. Under such a situation, it could become impossible to distinguish between the bulk water molecule outside bilayers and the freezable interlamellar water molecule located at the center of the interlamellar space. As a result, the DPPG bilayers are caused to separate from each other, resulting in a single lamellar apparently different from the multilamellar of the neutral lipids of PE and PC, as shown in Fig. 1.

References

[1] M. Kodama, T. Miyata, Colloids Surfaces 109 (1996) 283–289.
[2] M. Kodama, T. Miyata, Thermochim. Acta 267 (1995) 365–372.
[3] J.M. Boggs, Biochim. Biophys. Acta 906 (1987) 353–404.
[4] M. Kodama, H. Inoue, Y. Tsuchida, Thermochim. Acta 266 (1995) 373–384.
[5] H. Hauser, Biochim. Biophys. Acta 772 (1984) 37–50.
[6] G. Cevc, D. Marsh, Biophys. J. 47 (1985) 21–31.
[7] C.W. Rigell, C. de Saussure, E. Freire, Biochemistry 24 (1985) 5638–5646.
[8] M. Kodama, T. Miyata, Y. Takaichi, Biochim. Biophys. Acta 1169 (1993) 90–97.
[9] J.F. Nagle, M.C. Wiener, Biochim. Biophys. Acta 942 (1988) 1–10.
[10] M.C. Wiener, R.M. Suter, J.F. Nagle, Biophys. J. 55 (1989) 315–325.
[11] T.J. McIntosh, Biophys. J. 29 (1980) 237–246.
[12] H. Hauser, I. Pascher, R.H. Pearson, S. Sundell, Biochim. Biophys. Acta 650 (1981) 21–51.